arXiv:cond-mat/9711270v2 [cond-mat.soft] 20 Feb 1998

Weakly nonlinear investigation of the Saffman-Taylor problem in a rectangular Hele-Shaw cell

José A. Miranda[1] and Michael Widom[2]

Department of Physics, Carnegie Mellon University, Pittsburgh, PA 15213

Abstract

We analyze the Saffman-Taylor viscous fingering problem in rectangular geometry. We investigate the onset of nonlinear effects and the basic symmetries of the mode coupling equations, highlighting the link between interface asymmetry and viscosity contrast. Symmetry breaking occurs through enhanced growth of sub-harmonic perturbations. Our results explain the absence of finger tip-splitting in the early flow stages, and saturation of growth rates compared with the predictions of linear stability.

PACS numbers: 47.20.Ma, 47.20.Gv, 47.54.+r, 68.10.-m

[1]e-mail:01jamn@npd.ufpe.br

[2]e-mail:widom@andrew.cmu.edu

1 Introduction

Pattern formation occurs in many hydrodynamics settings. The Saffman-Taylor problem [1], in which two immiscible viscous fluids move in a narrow space between two parallel plates (the so-called Hele-Shaw cell), is a widely studied example where a fluid-fluid interface evolves [2]. The initially flat interface separating the two fluids can be destabilized by either a pressure gradient advancing the less viscous fluid against the more viscous one, or by gravity, as a result of a density difference between the fluids. The interface deforms, and different modes grow and compete dynamically leading to undulated patterns. The physics of the first stage of interface instability is captured by linear stability analysis [2]. After this initial linear behavior, the system evolves through a "weakly nonlinear" stage to a complicated late stage, characterized by formation of fingers and bubbles, in which nonlinear effects dominate.

The majority of analytical investigations of the dynamics of fingering instability focus on linear stability analysis or else on selection of steady-state patterns [2]. More recent analytical development [3] addresses the fully nonlinear time-evolving flow in the small surface tension limit. In contrast, our

present work develops an analytical approach which links the initial linear behavior with the strongly nonlinear advanced stages of the flow. We consider early stages of the flow, focusing especially on the onset of nonlinear effects. We employ an analytical approach known as a mode coupling theory, following the method of Haan [4] who studied the Rayleigh-Taylor instability in inertial confinement fusion. We previously applied this method to the Saffman-Taylor instability in radial flow geometry Hele-Shaw cells [5]. A closely related study in the context of solidification was carried out in reference [6]. Although our approach is quantitatively accurate only at early stages of pattern formation, we gain insight into the mechanisms of pattern selection and evolution.

For the rectangular flow geometry, numerical simulations [7, 8, 9, 10] and experiments [11, 12, 13] show that in the nonlinear regime, the viscosity contrast A (defined as the difference between the two fluid viscosities divided by their sum) plays a major role in the interface evolution. Most noteworthy is the role of viscosity contrast in breaking the symmetry of the interface. Linear stability analysis does not reveal any interface symmetry breaking in the rectangular geometry. In contrast, for the radial geometry the distinction

between inside and outside of the interface always breaks the symmetry.

For the rectangular geometry, in the case of zero viscosity contrast ($A = 0$), the flow is symmetric about the original flat interface position. On average, the fingers of one fluid penetrate the second fluid as much as fingers from the second fluid penetrate the first one. For nonzero viscosity contrast ($A \neq 0$), the less viscous fluid penetrates further into the more viscous one. The less viscous fluid fingers exhibit stronger length variation than the more viscous fluid fingers. For intermediate flow stages, the result is short fingers of the more viscous fluid inside the less viscous fluid, and long fingers of the less viscous fluid inside the more. In this case, the up-down interface symmetry is obviously broken. At late stages the long fingers may pinch off forming bubbles.

In references [7, 8, 9, 10] the mathematical description of the fingering dynamics is written in terms of nonlinear integro-differential equations. These equations cannot be solved exactly, and consequently the role of A in asymmetry development is primarily revealed by numerically solving these equations. A simple analytical description of it remains to be explicitly addressed.

In addition to the up-down symmetry breaking issue, other possible phe-

nomena like finger tip-splitting and growth saturation are worth investigating. We investigate the saturation of fast-growing modes. By saturation we mean a reduction of the exponential rate of growth. Numerical studies of Tryggvason and Aref [7, 8] exhibit a saturation for Saffman-Taylor flow. Here, we verify the saturation of growth at third order mode coupling, like that seen in the Rayleigh-Taylor instability [4, 14, 15].

Numerical simulations for rectangular geometry flow [16, 17] indicate that fingers undergo a type of tip-splitting instability in the late stages of interface evolution when the dimensionless surface tension parameter B [18] is sufficiently small. Experiments [19, 20, 21, 22], performed at very low B, observed that the fingers of the less viscous fluid split at their tips while penetrating the more viscous one. They also observed highly ramified fractal-like structures, which hardly resemble a Saffman-Taylor finger. Despite extensive numerical and analytical calculations (see, for example, reference [3]), considerable uncertainty surrounds the theoretical understanding of such splitting events. In contrast, for the radial flow geometry, finger tip-splitting is common experimentally, and it is predicted by a second-order mode coupling theory [5]. In this paper, we demonstrate that symmetries of the rectan-

gular flow remove a force driving tip-splitting at second order, explaining why it does not commonly occur in early stages of the flow. We investigate the possibility of finger tip-splitting at third order, but find that it does not occur.

Section 2 carries out our analytical weakly nonlinear investigation and derives a differential equation describing the early nonlinear evolution of the interface modes. In section 3, we interpret the results obtained in section 2. We identify and analyze the basic symmetries of the mode coupling differential equation. The differential equation exhibits the interface asymmetry discussed above, and its relation to the value of A. It also indicates the absence of finger tip-splitting and the existence of growth saturation at third order. We concentrate our attention on the coupling of a small number of modes. Section 4 presents our final remarks and perspectives.

2 The mode coupling differential equation

Consider two semi-infinite immiscible viscous fluids, flowing in a narrow gap of thickness b, in between two parallel plates (see figure 1). We assume that

b is smaller than any other length scale in the problem, and therefore the system is considered to be effectively two-dimensional. Denote the densities and viscosities of the lower and upper fluids, respectively as ρ_1, η_1 and ρ_2, η_2. The fluids are assumed to be incompressible, and the flows are assumed to be irrotational, except at the interface. Between the two fluids there exists a surface tension σ. Inject fluid 1 at constant external flow velocity $\vec{v}_\infty = v_\infty \hat{y}$ at $y = -\infty$ and withdraw fluid 2 at the same velocity at $y = +\infty$. We describe the system in a frame moving with velocity $\vec{v}_\infty$, so that the interface may deform, but it does not displace from $y = 0$ on the average. In order to include the acceleration of gravity $\vec{g}$, we tilt the cell so that the y axis lies at angle β from the vertical direction. During the flow, the interface has a perturbed shape described as $y = \zeta(x,t)$ over the range $0 \leq x \leq L$ in the comoving frame.

The early nonlinear evolution of the interface obeys a mode coupling equation. We extend Haan's work on the Rayleigh-Taylor problem [4] to the case of viscous flow in a Hele-Shaw cell. The analytic model we seek predicts the evolution of the interface perturbation amplitude $\zeta(x,t)$.

We begin by representing the net perturbation $\zeta(x,t)$ in the form of a

Fourier expansion

$$\zeta(x,t) = \sum_k \zeta_k(t) \exp(ikx), \tag{1}$$

where

$$\zeta_k(t) = \frac{1}{L} \int \zeta(x,t) \exp(-ikx) dx \tag{2}$$

denotes the complex Fourier mode amplitudes. Expansion (1) includes all possible modes k, with the exception of $k = 0$ since we are in a comoving frame. The wave vectors are constrained to lie on the x axis, but can be either positive or negative. We apply periodic boundary conditions in x limiting the wave number k to discrete allowed values $2\pi n/L$, for integer n. Experimental realization of the Saffman-Taylor flow in a cylindrical Hele-Shaw cell [13] showed that periodic boundary conditions are similar to the presence of physical sidewalls.

In the following paragraphs we use Fourier analysis to gain insight into the analytic structure of the flow dynamics. The Fourier approach is of particular interest, since despite its simplicity, it allows one to adopt the familiar physical ideas of modes and growth rates developed in the linear theory. Here we go beyond the level of linear stability analysis and analytically investigate the weakly nonlinear stage of the evolution.

Since we are interested in the early nonlinear behavior of the system, our first task is to derive a differential equation for ζ_k, correct to third order. The relevant hydrodynamic equation is Darcy's law [1, 2]

$$\eta_i(\vec{v}_i + \vec{v}_\infty) = -\frac{b^2}{12}\left\{\vec{\nabla}p_i - \rho_i(\vec{g}\cdot\hat{y})\hat{y}\right\}, \tag{3}$$

where $\vec{v}_i = \vec{v}_i(x,y)$ and $p_i = p_i(x,y)$ are, respectively, the velocity and pressure in fluids $i = 1$ and 2. Equation (3) derives from the Navier-Stokes equation by neglecting inertial terms, assuming a parabolic flow profile with vanishing velocity at the plates, and by averaging the velocity over the perpendicular direction to the $x-y$ plane.

Supplement equation (3) with the irrotational flow condition $\vec{\nabla}\times\vec{v}_i = 0$. Under this circumstance the velocity is given by $\vec{v}_i = -\vec{\nabla}\phi_i$, where ϕ_i represents the velocity potential in each of the fluids. Rewrite equation (3) in terms of velocity potentials and then integrate. After dropping an arbitrary constant of integration we write Darcy's law for velocity potential

$$\eta_i\phi_i = \frac{b^2}{12}\left\{p_i + \rho_i g y\cos\beta\right\} + \eta_i v_\infty y. \tag{4}$$

Rewrite equation (4) for each of the fluids and subtract the resulting

equations from each other to obtain the jump condition

$$A\left(\phi_1|_{y=\zeta}+\phi_2|_{y=\zeta}\right)-\left(\phi_1|_{y=\zeta}-\phi_2|_{y=\zeta}\right)=2\left\{\frac{b^2(p_2-p_1)}{12(\eta_1+\eta_2)}+Uy\right\} \tag{5}$$

where

$$A=\frac{\eta_2-\eta_1}{\eta_2+\eta_1} \tag{6}$$

is the viscosity contrast and

$$U=\frac{b^2(\rho_2-\rho_1)g\cos\beta}{12(\eta_1+\eta_2)}+Av_\infty \tag{7}$$

is a characteristic velocity of the problem. We concentrate attention on $U>0$, because there is no instability when $U<0$.

The pressure difference at the interface between the two fluids is given by [2]

$$(p_2-p_1)|_{y=\zeta}=\sigma\left(\frac{1}{R_\parallel}+\frac{1}{R_\perp}\right). \tag{8}$$

The two principal radii of curvature, $R_\parallel$ and $R_\perp$, describe the interface locally. The curvature in the $x-y$ plane is [23]

$$\kappa_\parallel=\frac{1}{R_\parallel}=\left(\frac{\partial^2\zeta}{\partial x^2}\right)\left[1+\left(\frac{\partial\zeta}{\partial x}\right)^2\right]^{-\frac{3}{2}}. \tag{9}$$

Meanwhile $R_\perp\sim b/2$, the radius of curvature in the direction perpendicular to the parallel plates, is controlled by the contact angle of the two-fluid interface at the plates. Typically, one finds that $R_\perp$ is nearly constant [24, 25].

Even though $1/R_\perp \gg 1/R_\parallel$, the perpendicular curvature does not significantly affect the motion in our problem, since its gradient is nearly zero.

Combine Darcy's law equation (5), with equations (8) and (9) for the pressure difference and rescale lengths by L and time by L/U, to obtain the dimensionless equation of motion

$$A\left(\phi_1|_{y=\zeta} + \phi_2|_{y=\zeta}\right) - \left(\phi_1|_{y=\zeta} - \phi_2|_{y=\zeta}\right) = 2\left[\zeta + B\kappa_\parallel\right]. \tag{10}$$

where

$$B = \frac{b^2\sigma}{12U(\eta_1+\eta_2)L^2} \tag{11}$$

is a dimensionless surface tension coefficient. From now on we work, unless otherwise stated, with the dimensionless equation of motion.

For our weakly nonlinear analysis we are interested in third order contributions in the perturbation amplitudes. Therefore, all the quantities in equation (10) are evaluated at the perturbed interface $y = \zeta(x,t)$, and not at the initial interface position $y = 0$ as is usually done in linearized surface deformation problems. The nonlinear terms arise because of this important distinction.

The incompressibility of the fluids ($\vec{\nabla}\cdot\vec{v}_i = 0$) means the velocity poten-

tials satisfy Laplace's equation $\nabla^2\phi_i = 0$. For points far from the interface, we expect uniform, steady flow uninfluenced by the interface. Therefore, we require that the system evolves with uniform velocity $\vec{v}_\infty = v_\infty\hat{y}$ in the limits $y \to \pm\infty$. Recall that $\vec{v}_i$ are measured in the comoving frame, and thus vanish at $y \to \pm\infty$. So, ϕ_1 and ϕ_2 go to constants (that we set to zero) as y goes to $-\infty$ and $+\infty$, respectively.

Now define Fourier expansions for the velocity potentials ϕ_i, which must obey Laplace's equation $\nabla^2\phi_i = 0$, the boundary conditions at $y \to \pm\infty$, and periodic boundary conditions on x. The general velocity potentials obeying these requirements are

$$\phi_1 = \sum_{k\neq 0} \phi_{1k}(t) \exp(|k|y) \exp(ikx), \tag{12}$$

and

$$\phi_2 = \sum_{k\neq 0} \phi_{2k}(t) \exp(-|k|y) \exp(ikx). \tag{13}$$

Substitute expansions (12) and (13) into the equation of motion (10). Keep third order terms in the perturbation amplitudes, and then Fourier transform. For example, the Fourier transform of the lower fluid velocity potential at

the perturbed interface $y = \zeta$ with wave vector k takes the form

$$\hat{\phi}_1(k) = \phi_{1k}(t) + \sum_{k' \neq 0} |k'| \phi_{1k'}(t) \zeta_{k-k'} + \frac{1}{2} \sum_{k', q \neq 0} (k')^2 \phi_{1k'}(t) \zeta_q \zeta_{k-k'-q}, \qquad (14)$$

where ζ_k is the Fourier expansion of ζ, given by equation (2). A similar expression for $\phi_2|_{y=\zeta}$ can be easily obtained. Likewise, the Fourier transform of the in-plane curvature with wave vector k, valid up to third order in ζ, is

$$\hat{\kappa}_{\parallel}(k) = -k^2 \zeta_k - \frac{3}{2} \sum_{k', q \neq 0} (k')^2 q [k - k' - q] \zeta_{k'} \zeta_q \zeta_{k-k'-q}. \qquad (15)$$

To close equation (10) we need additional relations expressing the velocity potentials in terms of the perturbation amplitudes. To find these, consider the kinematic boundary condition, which states that the normal components of each fluid's velocity at the interface equals the normal velocity of the interface itself [26], i.e.

$$\frac{\partial \zeta}{\partial t} = \left(\frac{\partial \zeta}{\partial x} \frac{\partial \phi_i}{\partial x} \right)_{y=\zeta} - \left(\frac{\partial \phi_i}{\partial y} \right)_{y=\zeta}. \qquad (16)$$

Expand equation (16) to third order in ζ and then Fourier transform. Solving for $\phi_{ik}(t)$ consistently to third order in ζ yields

$$\phi_{1k}(t) \;=\; -\frac{\dot{\zeta}_k}{|k|} + \sum_{k' \neq 0} sgn(kk') \dot{\zeta}_{k'} \zeta_{k-k'}$$

$$- \sum_{k',q\neq 0} \frac{kq}{|k|} sgn(k'q) \dot{\zeta}_{k'} \zeta_{q-k'} \zeta_{k-q} + \sum_{k',q\neq 0} \frac{k'}{|k|} \left(k - q - \frac{k'}{2} \right) \dot{\zeta}_{k'} \zeta_q \zeta_{k-k'-q} \tag{17}$$

and a similar expression for $\phi_{2k}(t)$. Here sgn denotes the sign function. For instance, $sgn(kk') = 1$ if $(kk') > 0$ and $sgn(kk') = -1$ if $(kk') < 0$. The overdot denotes total time derivative.

Substitute this last expression for $\phi_{1k}(t)$ into equation (14), and again keep only cubic terms in the perturbation amplitude (the same procedure must be repeated for fluid 2). For $k \neq 0$, Darcy's law (10) becomes the differential equation

$$\begin{aligned}
\dot{\zeta}_k &= \lambda(k)\zeta_k + A|k| \sum_{k'\neq 0} \left[1 - sgn(kk')\right] \dot{\zeta}_{k'} \zeta_{k-k'} \\
&+ \sum_{k',q\neq 0} |k||q| sgn(k'q) \left[1 - sgn(kq)\right] \dot{\zeta}_{k'} \zeta_{q-k'} \zeta_{k-q} \\
&+ \sum_{k',q\neq 0} k' \left[k - q - \frac{k'}{2} - \frac{|k'||k|}{2k'} \right] \dot{\zeta}_{k'} \zeta_q \zeta_{k-k'-q} \\
&- \frac{3}{2} B \sum_{k',q\neq 0} |k| (k')^2 q [k - k' - q] \zeta_{k'} \zeta_q \zeta_{k-k'-q},
\end{aligned} \tag{18}$$

where A is the viscosity contrast as defined in equation (6), B is the dimen-

sionless surface tension coefficient given in equation (11) and

$$\lambda(k) = |k|(1 - Bk^2) \tag{19}$$

is the linear growth rate.

Equation (18) is the mode coupling equation of the Saffman-Taylor problem for the rectangular geometry Hele-Shaw flow. It gives us the time evolution of the perturbation amplitudes ζ_k accurate to third order, conveniently written in terms of the two dimensionless parameters A and B. The first term on the right-hand side of equation (18) reproduces the linear stability analysis [1-3]. The second term, of great importance for understanding the interface asymmetry, represents second-order mode coupling. The remaining terms depict the third order contributions to the mode coupling equation. They lead to saturation of the growth compared with the linear equation of motion. Beyond third order, we anticipate that all even terms are multiplied by A, and B enters only into odd terms. In the following section we investigate the mode coupling equation (18) in more detail.

3 Discussion

We begin our discussion by analyzing the basic symmetries present in the Saffman-Taylor problem and considering how they constrain the form of the mode coupling equation (18). Then we look in detail at features of the interface morphology dictated by the first-, second- and third-order terms.

Several symmetry operations leave the Hele-Shaw cell invariant. Because of the periodic boundary conditions introduced in section 2, the cell is invariant under infinitesimal horizontal translations $T_x^\epsilon : (x, y) \to (x + \epsilon, y)$. Provided the cell is sufficiently long in the vertical direction, we may assume vertical translational symmetry $T_y^\epsilon : (x, y) \to (x, y + \epsilon)$. Additional symmetries of the cell are the vertical mirror $M_v : (x, y) \to (-x, y)$ and the horizontal mirror $M_h : (x, y) \to (x, -y)$.

However, for the Saffman-Taylor problem, the differing fluid densities and viscosities, the gravitational acceleration $\vec{g}$ and external flow $\vec{v}_\infty$ break the symmetry M_h. We define a new symmetry transformation of the Saffman-Taylor problem $\tilde{M}_h : (x, y, A, B) \to (x, -y, -A, B)$. Interchanging viscosities η_1 and η_2 reverses the sign of A (see equation (6)). To understand the transformation of B defined in equation (11) we must study the transformation

of U defined in equation (7). Interchanging the densities ρ_1 and ρ_2, and simultaneously reversing the direction of gravitational acceleration $\vec{g}$ leaves the first term of equation (7) for U invariant. Reversing the sign of A and simultaneously reversing the direction of external flow velocity $\vec{v}_\infty$ leaves invariant the second term of equation (7). Invariance of U implies invariance of B. Thus $\tilde{M}_h$ swaps the two fluids and reverses the direction of gravitational acceleration and external flow at the same time as it reflects the y coordinate.

The Fourier modes $\zeta_k \exp(ikx)$ are basis functions for representations of the symmetry group generated by the above operations. By investigating the transformation of modes under group generators we can check the symmetry properties of the mode coupling equation (18), and explain the presence and/or absence of various terms. For example, applying horizontal translation T_x^ϵ to a mode of wave vector k multiplies its coefficient ζ_k by the complex phase factor $\exp(ik\epsilon)$. All terms in the mode coupling equation must transform identically under this translation. Every product of coefficients $\prod_j \zeta_{k_j}$ gets multiplied by $\exp(i \sum_j k_j \epsilon)$. Consequently, the wave vectors k_j in each term must sum up to a common value, k. Inspection of equation (18) verifies this rule.

Applying vertical translation T_y^ϵ has no effect (the mode transforms as the identity) because $\zeta(x)$ is defined as the interfacial height *relative* to the unperturbed interface. Thus the vertical translation symmetry does not significantly constrain the form of equation (18).

The vertical mirror M_v reverses the sign of k. Invariance under this operation requires that ζ_{-k} obeys the same equation as ζ_k. Inspection of equation (18) confirms that all coefficients are even under the reversal of sign of all wave vectors. For example, expressions that are first or third order in the wave vectors are written as an even power of the wave vectors times an absolute value of a wave vector. The even symmetry of the coefficient $\lambda(k)$ is explicitly revealed in equation (19).

The horizontal mirrors (both M_h and $\tilde{M}_h$) reverse the sign of ζ_k. We will discuss the transformation of individual terms in equation (18) under these mirror operations in subsequent sections as we discuss evolution of the interface up to first-, second-, and third-order in our mode coupling theory.

3.1 First order - Linear evolution

The linear stability analysis of the viscous fingering problem has been studied since the late 50's [1, 2]. Due to its importance, we briefly review some features of the linear regime. Start with the first order solution to equation (18)

$$\zeta_k^{lin}(t) = \zeta_k(0) \exp[\lambda(k)t]. \tag{20}$$

The linear growth rate $\lambda(k)$ (see equation (19)), which leads to exponential growth at small amplitudes, is plotted in figure 2 for $B = 1$. From figure 2 we see that, for small wave vectors, perturbations grow in time, deforming the interface. At large wave vectors, surface tension stabilizes short wavelength deviations. From the linear growth rate (19) we can extract two important parameters: the critical wave vector (defined by setting $\lambda(k) = 0$)

$$k_c = \frac{1}{\sqrt{B}} \tag{21}$$

beyond which all modes are linearly stable; and the fastest growing mode (defined by setting $d\lambda(k)/dk = 0$)

$$k^* = \frac{1}{\sqrt{3B}}, \tag{22}$$

which dominates the initial dynamics of the interface. The fastest growing wavelength $\lambda^* = 2\pi/k^*$ sets a characteristic length to the problem, giving

the experimentally observed period of the fingering pattern at initial stages of the flow.

Consider the transformation of the first-order terms in our mode-coupling equation (18) under horizontal reflections. The coefficient ζ_k reverses sign on both sides of the equation. What about $\lambda(k)$? Since it depends only on constant parameters defining the system under study, independent of the shape of the interface, it exhibits invariance under M_h. As a result the linear analysis neither predicts, nor explains, the interface asymmetry observed in simulations [7, 8, 9, 10] and experiments [11, 12, 13]. Although at first-order the interface shapes remain (statistically) symmetric under M_h, the Saffman-Taylor problem does not respect M_h symmetry because of the distinction between the lower and upper fluids, and the directions of gravitational acceleration and external flow. The symmetry operation $\tilde{M}_h$ is the appropriate symmetry for the Saffman-Taylor problem. Since B is invariant under $\tilde{M}_h$, so is the linear growth rate $\lambda(k)$, confirming the required symmetry.

It is convenient to rewrite the net perturbation (1) in terms of cosine and sine modes

$$\zeta(x,t) = \sum_{k>0} \left[a_k(t)\cos(kx) + b_k(t)\sin(kx) \right], \tag{23}$$

where $a_k = \zeta_k + \zeta_{-k}$ and $b_k = i\,(\zeta_k - \zeta_{-k})$ are real-valued. Tryggvason and Aref [8] studied the nonlinear behavior of the interface numerically, considering the interaction between two cosine waves. Similarly, to illustrate the linear evolution of the interface, we perturb the initially flat interface with two cosine modes a_{k_s} and a_{k_f}. We consider a dominant *fundamental* wave of wave vector $k_f = k^* = 1/\sqrt{3}$ and initial amplitude $a_{k_f}(0)$, and a second *sub-harmonic* wave of wave vector $k_s = k_f/2$ and relatively weak amplitude $a_{k_s}(0) = 0.2a_{k_f}(0)$.

Exactly two wavelengths of the fundamental mode fit in the Hele-Shaw cell, so the fundamental mode is invariant under horizontal translations $T_x^{L/2}$. The sub-harmonic perturbation a_{k_s} breaks this translational symmetry of the fundamental perturbation a_{k_f} by slightly altering the relative lengths of the two upward-pointing fingers. Up-down symmetry of the interface is weakly broken, by construction, due to our arbitrary choice of sub-harmonic $a_{k_s}\cos(k_s x)$. Had we taken the sub-harmonic $b_{k_s}\sin(k_s x)$ instead, the length alternation would have appeared in the downward-pointing fingers.

Figure 3a depicts the interface given by linear theory. We observe that the interface remains nearly up-down symmetric, showing no particular tendency

to interface asymmetry development. Each uncoupled mode by itself respects up-down symmetry. The translational and reflection symmetry breaking of the interface are artifacts of the particular initial condition we select. The interfacial deformation grows sufficiently large that quantitative accuracy of any perturbative approach is doubtful. We illustrate such large amplitudes deliberately, however, because they enhance the visibility of nonlinear effects described in the next two subsections.

3.2 Second order - Role of the asymmetry parameter A

For sufficiently short times we presume that the perturbation series defining the mode coupling equation of motion, and its solutions, converge to their true forms as successively higher-order terms are incorporated. Truncating equation (18) at second order should then result in quantitatively small changes in the calculated interface profile $\zeta(x,t)$. Although quantitatively small, these changes should incorporate the principal corrections to the linear interface evolution discussed above in section 3.1. Indeed, this section explains two important qualitative features of the interfacial evolution: up-

down symmetry breaking, and the general absence of finger splitting.

We consider first the breaking of up-down symmetry. As noted above, in section 3.1, the linear evolution respects reflection symmetry M_h since ζ_k reverses sign on both sides of the equation of motion, while $\lambda(k)$ is unaffected. In contrast, the second order term in equation (18) breaks M_h symmetry because it does not change sign. The second order term is multiplied by the viscosity contrast A. Hence the breaking of up-down symmetry depends upon the difference between the viscosities of the two fluids. In equation (18) the role of A in asymmetry development is clearly identified, being revealed without solving any complicated nonlinear integro-differential equations [7, 8, 9, 10]. Our mode coupling approach provides a transparent and simple way of identifying the intrinsically nonlinear character of the viscosity contrast A.

Symmetry breaking in the equation of motion translates into symmetry breaking in the solution. We now solve equation (18) to second order accuracy. Substitute the linear solution (20) into the second-order terms on the right hand side of equation (18), to obtain

$$\begin{aligned}\dot{\zeta}_k &= \lambda(k)\zeta_k \\ &+ |k|A\sum_{k'\neq 0}\left[1-sgn(kk')\right]\lambda(k')\zeta_{k'}(0)\zeta_{k-k'}(0)\exp[(\lambda(k-k')+\lambda(k'))t] \\ &+ \mathcal{O}(\zeta_k^3), \end{aligned} \tag{24}$$

where $\lambda(k-k')$ and $\lambda(k')$ are the linear growth rates related to the modes $k-k'$ and k', respectively. Equation (24) is a standard first order differential equation [27] with the solution

$$\zeta_k = \zeta_k^{lin} + |k|A\sum_{k'\neq 0}\zeta_{k'}(0)\zeta_{k-k'}(0)\mathcal{G}(k,k',t) + \mathcal{O}(\zeta_k^3), \tag{25}$$

where

$$\begin{aligned}\mathcal{G}(k,k',t) &= \left[1-sgn(kk')\right]\left(\frac{\lambda(k')}{\lambda(k-k')+\lambda(k')-\lambda(k)}\right) \\ &\times \left(\exp[\lambda(k-k')+\lambda(k')]t - \exp[\lambda(k)t]\right). \end{aligned} \tag{26}$$

The apparent singularities in $\mathcal{G}(k,k',t)$ at $\lambda(k)=\lambda(k')+\lambda(k-k')$ are cancelled by zeros in the numerator of (26), and each term in the sum (equation (25)) is regular at these points. At this apparent "resonance point" $\mathcal{G}(k,k',t)$ varies as $t\exp[\lambda(k)t]$.

We use the second order solution (25) to investigate the coupling of a small number of modes. As discussed in reference [8], even the interaction of

two modes can lead to patterns relevant to more complex statistical-fingering calculations [7]. Our discussion will be simpler if we replace the complex Fourier modes ζ_k with sine and cosine modes as in equation (23). The second order equations of motion are

$$\dot{a}_k = \lambda(k) a_k + Ak \sum_{k'>0} \left[\dot{a}_{k'} a_{k+k'} + \dot{b}_{k'} b_{k+k'} \right], \tag{27}$$

$$\dot{b}_k = \lambda(k) b_k + Ak \sum_{k'>0} \left[\dot{a}_{k'} b_{k+k'} - \dot{b}_{k'} a_{k+k'} \right]. \tag{28}$$

Note how the products of sine and cosine amplitudes are arranged to preserve the M_v symmetry under which the sine functions are odd and the cosines are even. Solutions to these equations are similar in form to (25).

Figure 3b illustrates the second-order solution taking the same two-mode initial conditions used in figure 3a. Since $k_s = k_f/2$, equations (27) and (28) couple the growth of the sub-harmonic to the amplitude of the fundamental. Finger competition, associated with the sub-harmonic mode, is enhanced to a degree proportional to the viscosity contrast A. Figure 3b represents the extreme case $A = 1$. Length variation between the upwards fingers is stronger than in figure 3a. Notice also that the central upward finger advances more strongly into the upper fluid than the downward fingers into the lower fluid.

The upward finger at $x = 0$ advances less strongly.

Mode coupling not only influences the *magnitude* of the sub-harmonic, but also selects its *phase*. Without loss of generality we may take $a_{k_f} > 0$ and $b_{k_f} = 0$, as we do in the initial conditions for figure 3b. Now compare the growth rates of sine and cosine sub-harmonic modes

$$\dot{a}_{k_s} = \lambda(k_s) a_{k_s} + A k_s \dot{a}_{k_s} a_{k_f}, \tag{29}$$

$$\dot{b}_{k_s} = \lambda(k_s) b_{k_s} - A k_s \dot{b}_{k_s} a_{k_f}. \tag{30}$$

Positive viscosity contrast $A > 0$ increases the growth rate of the cosine sub-harmonic a_{k_s}, causing increased variability among the lengths of fingers of the less viscous lower fluid 1 penetrating downwards into the more viscous upper fluid 2. Note that the sign of a_{k_s} is dictated by initial conditions, and not influenced by mode-coupling. Reversing the sign of a_{k_s} has the effect of interchanging which of the two upwards pointing fingers will grow at the expense of the other. This is tantamount to a horizontal translation by $L/2$. Finally consider patterns with $a_{k_s} = 0$ and $b_{k_s} \neq 0$. Inspecting equation (30) we see that $A > 0$ inhibits the growth of sine modes b_{k_s}. Sine modes would vary the lengths of fingers of the more viscous upper fluid 2 penetrating into

the less viscous lower fluid 1, but their growth is inhibited.

Reversing the sign of A exactly reverses the above conclusions. Sub-harmonic sine modes will be favored over cosine modes. This happens because of the $\tilde{M}_h$ invariance of the Saffman-Taylor problem. Reversing the signs of both $\zeta(x)$ and A leaves the form of equation (18) invariant. Consequently, a randomly chosen up-down symmetric (on average) initial condition always evolves into a symmetry-broken interfacial pattern in which the fingers of the less viscous fluid exhibit variable finger lengths penetrating into the more viscous fluid [1, 11, 12, 13].

Further inspection of the cosine and sine mode coupling equations (27) and (28) reveals that, while the presence of large wave number modes influences the growth of smaller wave number modes, the reverse is not true. For example, the growth of any mode k cannot be influenced (up to second order) by modes of only smaller wave numbers. In particular, there is no second order term entering the equation of motion for the fundamental mode k_f in the presence of the sub-harmonic k_s. Likewise the presence of $k_f = k^*$ and $k_s = k_f/2$ cannot alter the evolution of the *harmonic* mode $k_h = 2k_f$. Since $k_h > k_c$, the harmonic mode is linearly stable ($\lambda(k_h) < 0$) and will not

spontaneously grow.

This observation yields insight into the absence of finger tip-splitting in the rectangular geometry Saffman-Taylor problem, at second order. Splitting the tips of the fingers in figure 3b would require the presence of a sizable harmonic mode of wave number k_h. Even if such modes enter weakly through initial conditions or random noise, they quickly die out.

This is in striking contrast to the radial geometry Saffman-Taylor problem [5], where mode coupling drives the growth of harmonic modes. In the radial case we may talk about the fundamental cosine mode number n_f, where n_f is an integer counting the number of oscillations around the growing perimeter. The influence of a fundamental mode n_f on the growth of its harmonic mode $n_h = 2n_f$ is given by the equation of motion [5]

$$\dot{a}_{n_h} = \lambda(n_h) a_{n_h} + \mathcal{C} a_{n_f}^2, \tag{31}$$

where $\lambda(n_h)$ denotes the linear growth rate related to the mode (n_h) in the radial geometry case, and $\mathcal{C}$ is negative. Even if $\lambda(n_h) < 0$, the harmonic mode can still grow provided the fundamental mode is present, $a_{n_f} \neq 0$. In the radial geometry the presence of the fundamental forces growth of the harmonic, while in the rectangular geometry the fundamental does not

influence the harmonic at second order. Because $\mathcal{C} < 0$, a_{n_h} is driven negative, the sign that is required to cause fingers to split.

Consider the behavior of the coefficient of $a_{n_f}^2$ under the radial analogue of $\tilde{M}_h$ (here denoted by $\tilde{M}_h^{radial}$), which interchanges the two fluids and reverses the direction of external flow while reversing the sign of the interfacial perturbation ζ. The coefficient, $\mathcal{C}$, contains both even and odd terms under $\tilde{M}_h^{radial}$. However, the odd terms are vanishingly small compared to the even terms for large unperturbed radii of curvature. We will treat $\mathcal{C}$ as effectively even under $\tilde{M}_h^{radial}$ in the discussion.

To transform consistently under $\tilde{M}_h^{radial}$, the radial equation of motion (31) must contain only terms that are odd. The second order term, however, is even and thus breaks $\tilde{M}_h^{radial}$ symmetry. This is expected, because $\tilde{M}_h^{radial}$ is not a symmetry of the radial flow Saffman-Taylor problem. The interface is always in-out asymmetric in radial flow because we can always distinguish the region of space that lies inside the interface from the region that lies outside. For instance, the outward radial motion in which air pushes oil in a radial Hele-Shaw cell (divergent flow) is not equivalent to the inward radial motion corresponding to withdrawal of oil surrounded by air (convergent

flow) [28]. This broken symmetry allows finger tip-splitting.

In contrast, $\tilde{M}_h$ *is* a symmetry of the *rectangular* Saffman-Taylor problem. Thus, even terms in the equation of motion, like the one that causes tip-splitting in the radial geometry, are forbidden in the rectangular geometry. Indeed, it can be shown that the amplitudes of these terms vanish when taking the rectangular geometry (large radius) limit of the radial flow equations of motion [5]. At second order the driving force creating finger tip-splitting is eliminated by the special symmetry of the rectangular geometry.

While $\tilde{M}_h$ rules out terms like $\mathcal{C}a_{k_f}^2$ with $\mathcal{C}$ even under $\tilde{M}_h$, it does not rule out similar terms with odd coefficients such as the viscosity contrast A. From our mode coupling equations (29) and (30) we know they are absent, because small wave number modes do not influence the growth of large wave number modes. We lack a symmetry explanation for why this is so.

Intermediate cases, between radial and rectangular flow geometry, are provided by the wedge geometry [28, 29, 30]. In the wedge geometry the fluids flow in a Hele-Shaw cell in which the side walls form a wedge with an opening angle of θ_0 ($-2\pi \leq \theta_0 \leq 2\pi$), where $\theta_0 > 0$ ($\theta_0 < 0$) corresponds to a divergent (convergent) flow. Experiments in the wedge geometry [28]

with $A > 0$ observed an increasing sensitivity to finger tip-splitting for larger angle $\theta_0 > 0$. A related experiment [28] with $A < 0$ and convergent flow shows that fingers grow, but tip-splitting of inward fingers is inhibited. At second order, the specially symmetric case $\theta_0 = 0$ is unique in the absence of a driving force leading to tip splitting.

3.3 Third order - Onset of saturation and absence of tip-splitting

Now we examine the whole third order mode coupling equation (18), taking into account the contributions coming from the third order terms. Since the final expressions are somewhat complicated, we start our discussion by considering the evolution of a single mode. The third order mode coupling equation (18) reduces to

$$\dot{\zeta}_k = \lambda(k)\zeta_k + k^3 \left[\frac{5}{2}Bk^2 - 1\right] \zeta_k^3, \tag{32}$$

where we have replaced $\dot{\zeta}_k$ with $\lambda(k)\zeta_k$ in terms already of third order on the right hand side of equation (18). Since we are interested in the fastest growing mode $k = k^* = 1/\sqrt{3B}$, we see from (32) that the third order terms

lead to a saturation of the growth because the coefficient of ζ_k^3 is negative. The exponential growth of the linear instability does not proceed unchecked.

Figure 3c illustrates the full solution up to third order of equation (18), taking the same initial conditions as were used in figures 3a and 3b, and including modes $a_{k_f/2}$ and a_{k_f}. The main effect that is apparent, in comparison with figure 3b, is significantly diminished amplitude of the fundamental mode a_{k_f} caused by the saturation effect described by equation (32). There is a slightly increased amplitude of the sub-harmonic a_{k_s}. We also note a slight broadening of the dominant central finger, and narrowing of the smaller finger at $x = 0$.

It is interesting to investigate the possibility of finger tip-splitting at third order. Finger tip-splitting is associated to the magnitude of the harmonic mode $2k_f$. It turns out that, at third order the cosines modes a_{k_f} and $a_{k_f/2}$ force growth of modes a_{2k_f} and $a_{3k_f/2}$. We consider initial conditions similar to those used in figures 3a-c, assuming that modes k_f, $k_s = k_f/2$ are initially present. We study how these two initial modes force growth of modes $2k_f$ and $3k_f/2$. The influence of the fundamental and sub-harmonic on the growth of

the first harmonic $k_h = 2k_f$ may be expressed by

$$\dot{a}_{k_h} = \lambda_{eff} a_{k_h} - \frac{3}{8} B k_h k_s^2 k_f \left[k_f + 2k_s\right] a_{k_f} a_{k_s}^2 + \mathcal{O}(a_{k_h}^3), \tag{33}$$

where

$$\lambda_{eff} = \lambda(k_h) + \frac{k_f^2 k_h}{2}\left[B\left(k_f^2 + \frac{3}{2}k_h^2\right) - 1\right] a_{k_f}^2 + \frac{k_s^2 k_h}{2}\left[B\left(k_s^2 + \frac{3}{2}k_h^2\right) - 1\right] a_{k_s}^2. \tag{34}$$

In equation (33), the linear growth rate of mode k_h is increased by the presence of k_f and k_s. Although $\lambda(k_h)$ is negative, opposing the growth of the harmonic, the fundamental and sub-harmonic make λ_{eff} less negative. Quantitatively, the role of the fundamental dominates the sub-harmonic in increasing λ_{eff}.

It appears at a glance in equation (34) that sufficiently large a_{k_f} drives λ_{eff} positive, permitting growth of the harmonic a_{k_h}. It turns out that is an artifact of truncating the mode coupling theory. If higher order terms in a_{k_f} are kept, λ_{eff} will remain negative. Terms involving a_{k_f} and a_{k_s} make λ_{eff} less negative but cannot make it go positive. The physical reason that prevents positive values for λ_{eff} can be understood by considering the contour length of the interface. Introducing the harmonic always increases

the contour length, although the larger the amplitude of the fundamental, the smaller the increase upon introducing the harmonic. Multiplying the contour length by the surface tension yields surface energy that favors minimum contour length.

There will be a small amplitude of the harmonic present due to the driving term proportional to $a_{k_f} a_{k_s}^2$ in equation (33), but it is doubtful the amplitude will be sufficiently large to split the fingers, because it varies like the second power of the sub-harmonic. Therefore, no finger tip-splitting is observed even at third order.

A possible exception to this rule arises from a nonlinear instability caused by the coupling of the harmonic mode to itself. Inspecting equation (32) we note that high wavenumber modes with $k > \sqrt{2/5B}$ (the harmonic mode satisfies this condition) are unstable for sufficiently large amplitude, because the coefficient of ζ_k^3 is positive. This large-amplitude instability was previously noted in the related solidification problem by Dee and Mathur [6]. Finger tip-splitting in the Saffman-Taylor problem, induced by large amplitude noise assisted by a nonlinear instability, has been suggested on the basis of numerical simulations [16, 17] and seen in experiments [19, 20, 21, 22], performed

at very low B.

4 Concluding remarks

In this paper we developed a mode coupling theory to investigate the onset of nonlinear effects in the viscous fingering problem in a rectangular Hele-Shaw cell. From a weakly nonlinear analysis of the system, we derived a mode coupling differential equation which describes the evolution of the interface perturbation amplitudes. The basic symmetries of the mode coupling equation are identified and discussed.

We investigated the relation between the viscosity contrast A and the interfacial asymmetry in the Saffman-Taylor problem. Viscosity contrast A multiplies symmetry-breaking terms in the mode coupling equation. Our analysis explicitly indicates that symmetry breaking occurs through enhanced growth of sub-harmonic perturbations. We show that second-order terms that drive tip-splitting in the radial flow geometry are prohibited by symmetry, explaining the general absence of tip-splitting in the rectangular geometry. A remaining mystery is to explain why small wave number modes do

not alter the growth of high wave number modes at second order.

Our mode coupling analysis shows that modest growth of the harmonic may occur at third order by a reduction of the effective linear stability of the harmonic mode, coupled with a driving process assisted by finger competition. We do not expect this process to result in finger tip-splitting under normal circumstances. However, self-coupling of the harmonic creates a nonlinear instability that could split finger tips if noise or other factors drive a sufficiently large harmonic amplitude. Finally, we identified the onset of saturation effects, which moderates the exponential growth of the linear instability.

In a separate work [31] we extend the present theory to a system in which one of the two fluids is a ferrofluid [26], and a magnetic field is applied normal to the Hele-Shaw cell. Interfacial symmetry breaking at late stages is very dramatic in this system [32]. We point out, here, that the onset of interface symmetry breaking depends on viscosity contrast A, not on the applied magnetic field. In reference [31] we show that finger tip-splitting arises as a result of the application of an external magnetic field.

Acknowledgments

J.A.M. (CNPq reference number 200204/93-9) would like to thank CNPq (Brazilian Research Council) for financial support. This work was supported in part by the National Science Foundation grant No. DMR-9221596.

References

[1] P. G. Saffman and G. I. Taylor, Proc. R. Soc. London Ser. A **245**, 312 (1958).

[2] For review articles on this subject, see D. Bensimon, L. P. Kadanoff, S. Liang, B. I. Shraiman and C. Tang, Rev. Mod. Phys. **58**, 977 (1986); G. Homsy, Ann. Rev. Fluid Mech. **19**, 271 (1987); S. D. Howison, Eur. J. Appl. Math. **3**, 209 (1992); K. V. McCloud and J. V. Maher, Phys. Rep. **260**, 139 (1995).

[3] M. Siegel, S. Tanveer and W.-S. Dai, J. Fluid Mech. **323**, 201 (1996) and references therein; S. Tanveer, Phil. Trans. R. Soc. Lond. A **343**, 155 (1993).

[4] S. W. Haan, Phys. Fluids B **3**, 2349 (1991).

[5] J. A. Miranda and M. Widom, "Radial fingering in a Hele-Shaw cell: a weakly nonlinear analysis", to appear in Physica D (1998).

[6] G. Dee and R. Mathur, Phys. Rev. B **27**, 7073 (1983).

[7] G. Tryggvason and H. Aref, J. Fluid Mech. **136**, 1 (1983).

[8] G. Tryggvason and H. Aref, J. Fluid Mech. **154**, 287 (1985).

[9] J. Casademunt, D. Jasnow and A. Hernández-Machado, Int. J. Mod. Phys. B **6**, 1647 (1992).

[10] J. Casademunt and D. Jasnow, Phys. Rev. Lett. **67**, 3677 (1991); J. Casademunt and D. Jasnow, Physica D **79**, 387 (1994).

[11] J. V. Maher, Phys. Rev. Lett. **54**, 1498 (1985).

[12] M. W. DiFrancesco and J. V. Maher, Phys. Rev. A **39**, 4709 (1989); M. W. DiFrancesco and J. V. Maher, Phys. Rev. A **40**, 295 (1989).

[13] H. Zhao and J. V. Maher, Phys. Rev. A **42**, 5894 (1990).

[14] S. W. Haan, Phys. Rev. A **39**, 5812 (1989).

[15] R. P. J. Town, J. D. Findlay and A. R. Bell, Laser Part. Beams **14**, 237 (1996).

[16] A. J. DeGregoria and L. W. Schwartz, J. Fluid Mech. **164**, 383 (1986).

[17] E. Meiburg and G. M. Homsy, Fluids **31**, 429 (1988).

[18] The dimensionless surface tension parameter B (defined in equation (11)) is a measure of the surface tension forces relative to viscous forces. A low value of B would mean, for instance, small surface tension or high speeds of flow.

[19] C. -W. Park and G. M. Homsy, Phys. Fluid **28**, 1583 (1985).

[20] P. Tabeling, G. Zocchi and A. Libchaber, J. Fluid Mech. **177**, 67 (1987).

[21] T. Maxworthy, J. Fluid Mech. **177**, 207 (1987).

[22] A. Arnéodo, Y. Couder, G. Grasseau, A. Hakim and M. Rabaud, Phys. Rev. Lett. **63**, 984 (1989).

[23] B. A. Dubrovin, A. T. Fomenko, and S. P. Novikov, *Modern Geometry-Methods and Applications, Part 1* (Springer-Verlag, New York, 1984).

[24] J. W. McLean and P. G. Saffman, J. Fluid Mech. **102**, 455 (1981); P. G. Saffman, in *Macroscopic Properties of Disordered Media*, 1982, Lecture Notes in Physics, vol. **154**, p. 208, edited by R. Burridge, S. Childress and G. Papanicolaou (Springer-Verlag, New York, 1982).

[25] For a discussion on the influence of wall wetting effects on $R_\perp$, see C. -W. Park and G. M. Homsy, J. Fluid Mech. **139**, 291 (1984); D. A. Reinelt, J. Fluid Mech. **183**, 219 (1987).

[26] R. E. Rosensweig, *Ferrohydrodynamics* (Cambridge University Press, Cambridge, 1985), and references therein.

[27] I. S. Gradshteyn and I. M. Ryzhik, *Table of Integrals, Series, and Products* (Academic Press, New York, 1994).

[28] H. Thomé, M. Rabaud, V. Hakim and Y. Couder, Phys. Fluids **A1**, 224 (1989).

[29] M. Ben Amar, Phys. Rev. A **44**, 3673 (1991).

[30] Y. Tu, Phys. Rev. A **44**, 1203 (1991).

[31] M. Widom and J. A. Miranda, "Viscous fingering patterns in ferrofluids", submitted to J. Stat. Phys. (1998).

[32] R. Perzynski et. al (unpublished).

Figure Captions

Figure 1: Schematic configuration of the flow in a rectangular Hele-Shaw cell. The densities and viscosities of lower and upper fluids are ρ_1, η_1 and ρ_2, η_2, respectively. The dashed line represents the unperturbed interface $y = 0$ and the solid undulated curve depicts the perturbed interface $y = \zeta(x, t)$, over the range $0 \leq x \leq L$. The surface tension between the two fluids is given by σ and the gravitational acceleration, directed in the negative vertical direction, is denoted by $\vec{g}$. The Hele-Shaw cell of thickness b is tilted by an angle β from the vertical direction. $\vec{v}_\infty = v_\infty \hat{y}$ represents the uniform overall velocity.

Figure 2: Linear growth $\lambda(k)$ [see equation (19) in the text] as a function of the wave number k, for $B = 1$. The critical wave number $k_c = \pm 1$, and the most unstable wave number $k^* = \pm 1/\sqrt{3}$.

Figure 3: Time evolution of the interface between the fluids, for the case of two interacting cosine waves. The dominant mode wave vector $k_f = k^* =$

$1/\sqrt{3}$ has initial perturbation amplitude $a_{k_f}(0)$=1. The sub-harmonic mode wave vector $k_s = k_f/2$ and initial amplitude $a_{k_s}(0) = 0.2a_{k_f}(0)$. For all panels the vertical axis scale is the same, the parameter $B = 1$, and t=0, 1.5, 3.0 and 4.5; (a) First order (linear) solution; (b) Second order solution for $A = 1$; (c) Third order solution for $A = 1$.

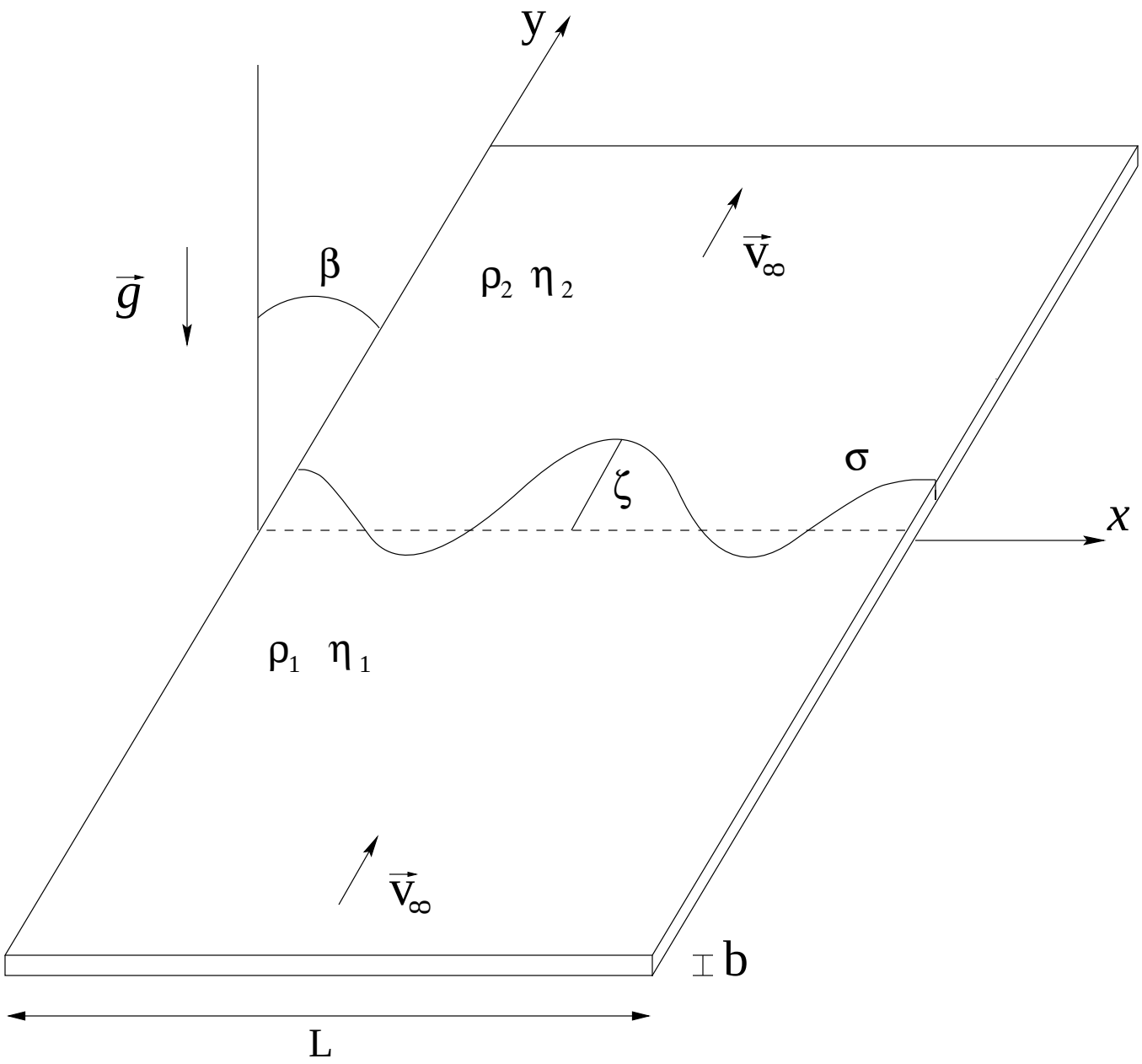

Figure 1

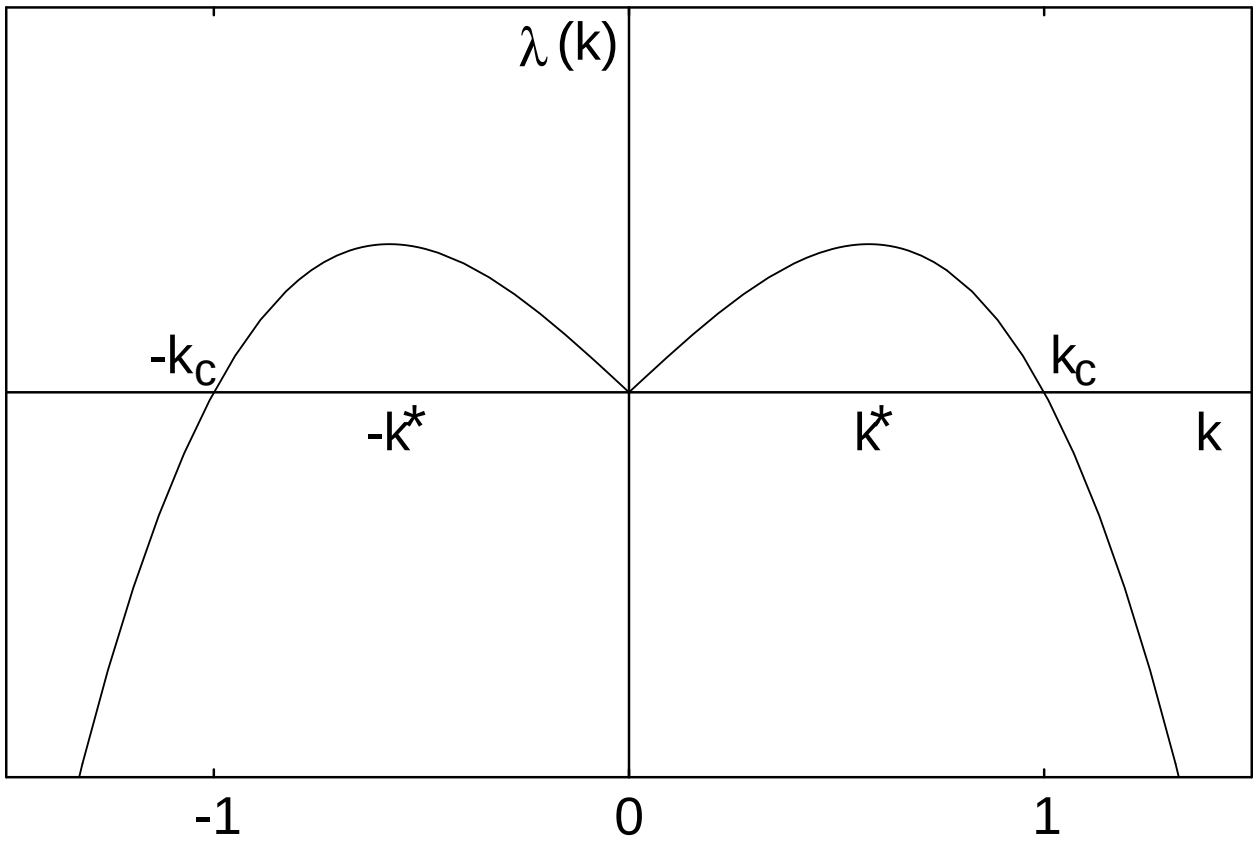

FIGURE 2

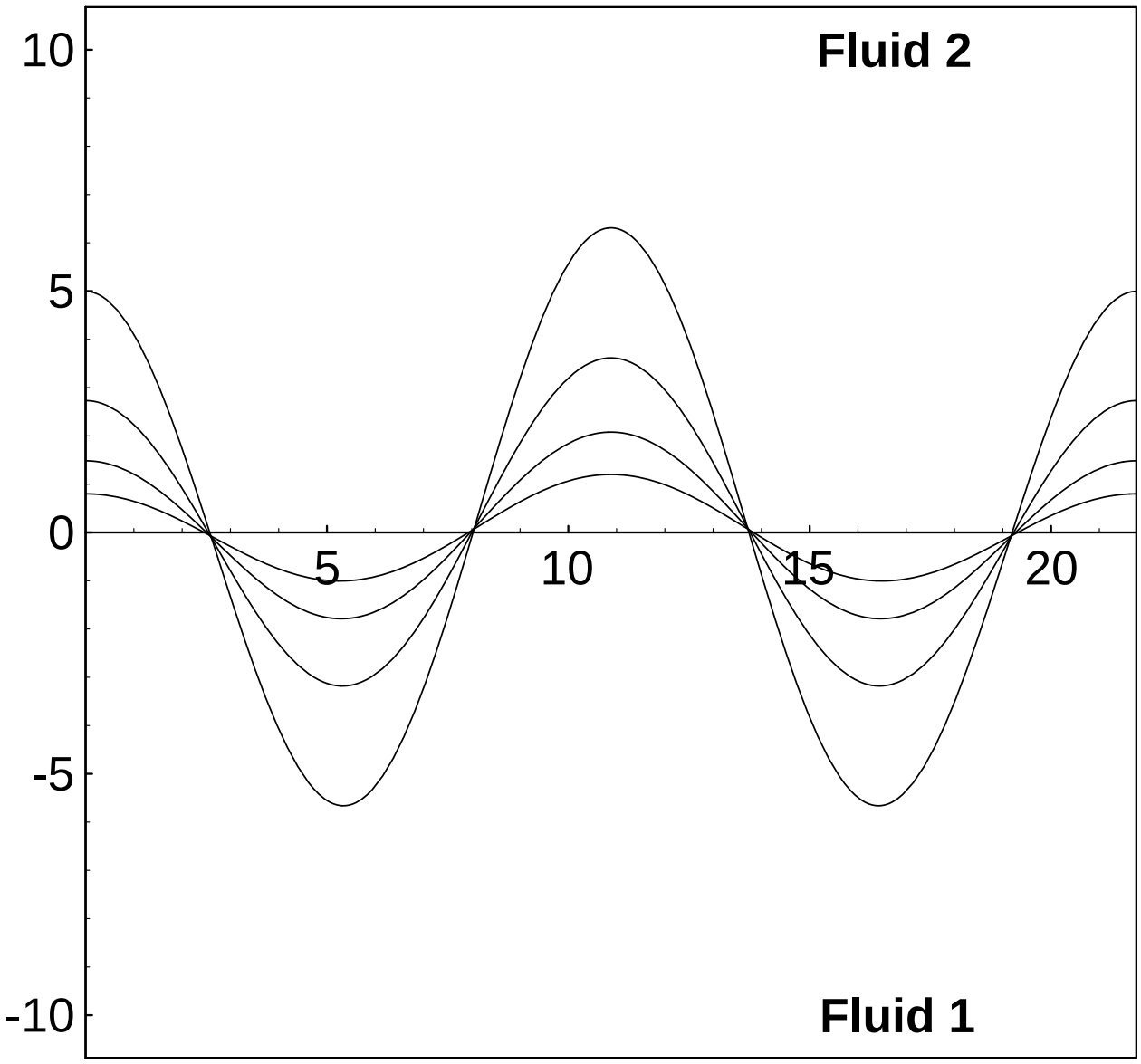

FIGURE 3(a)

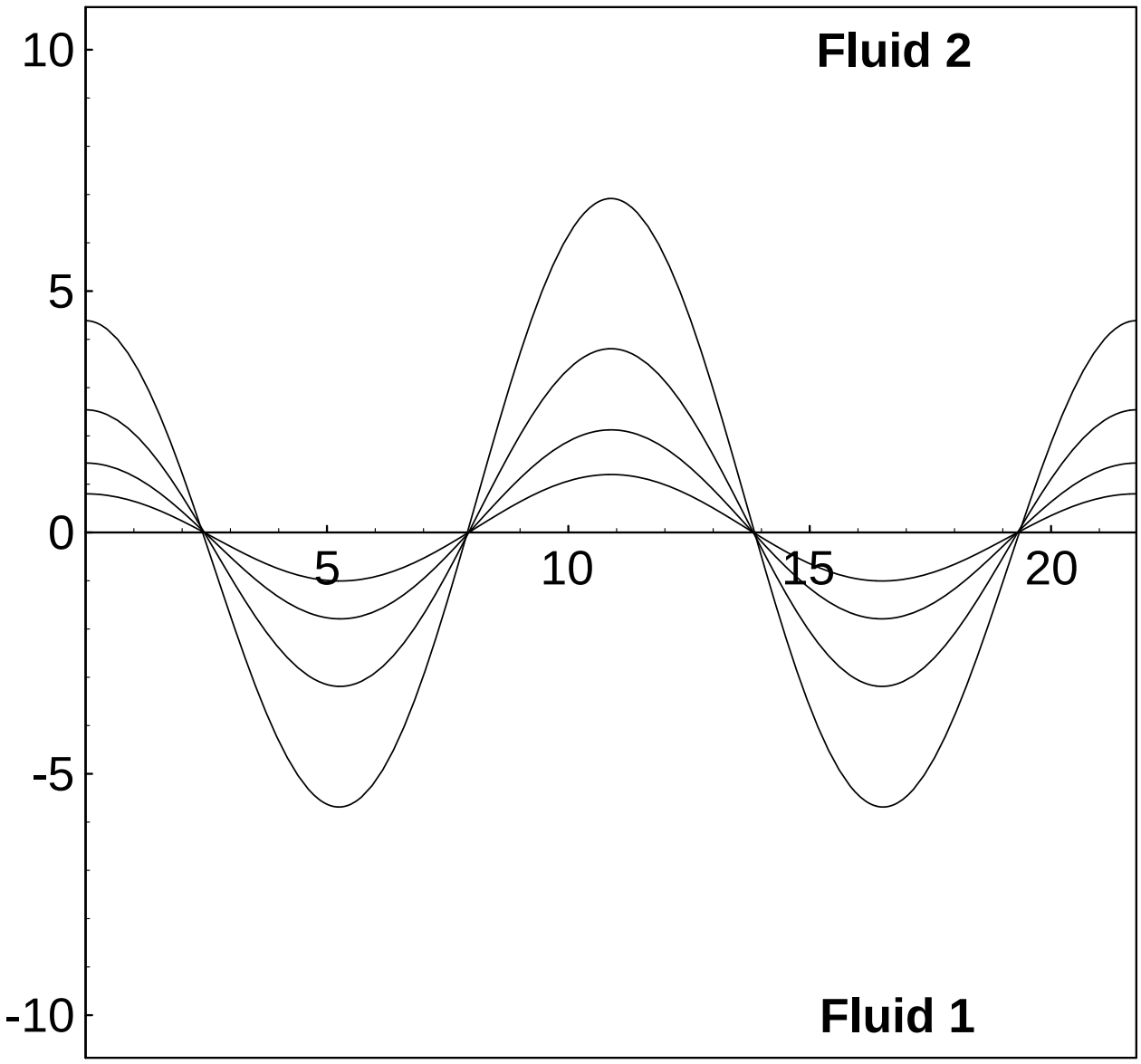

FIGURE 3(b)

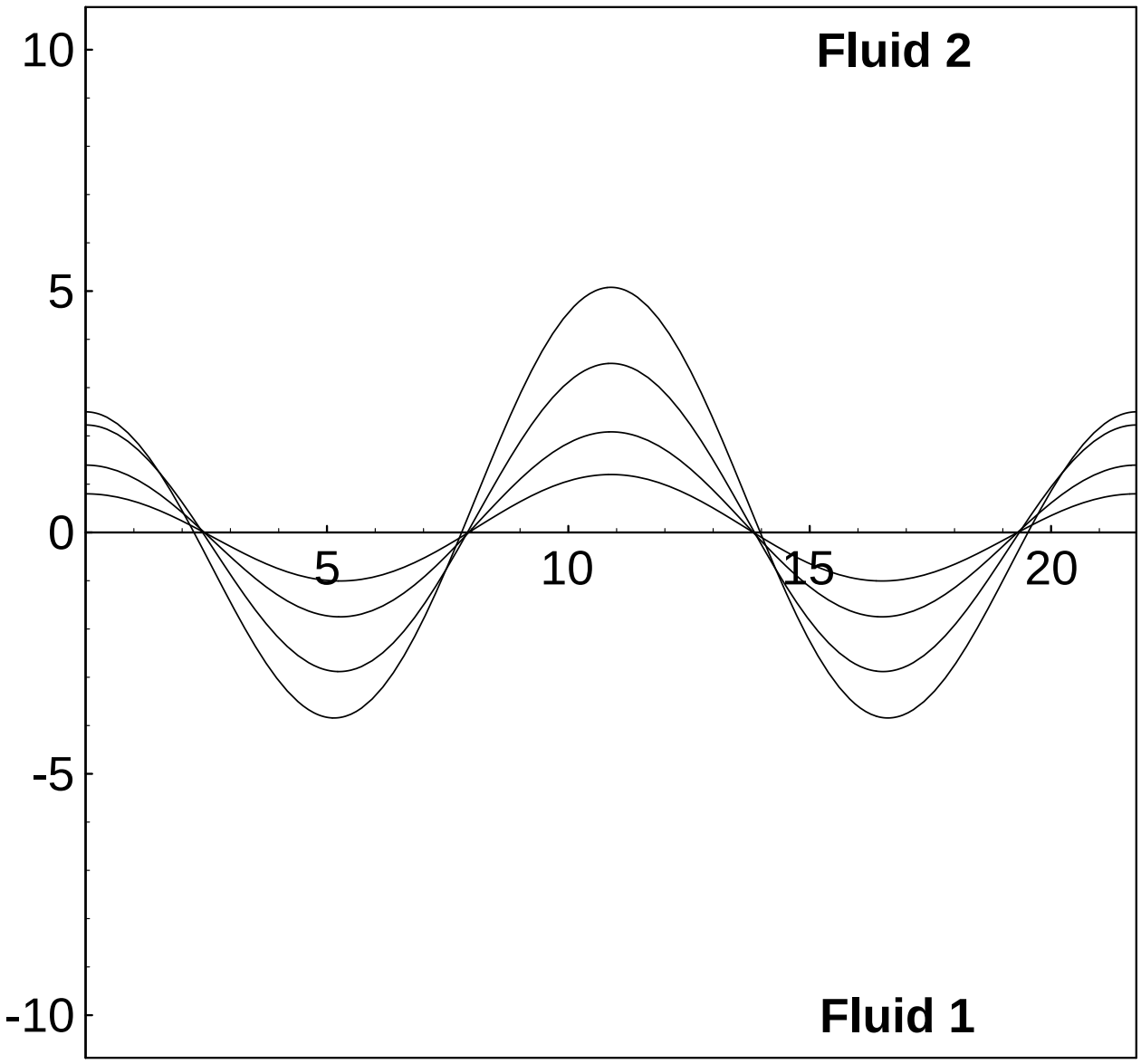

FIGURE 3(c)